Magnesium Technology 2011
Edited by: Wim H. Sillekens, Sean R. Agnew, Neale R. Neelameggham, and Suveen N. Mathaudhu
TMS (The Minerals, Metals & Materials Society), 2011

Small Fatigue Crack Growth Observations in an Extruded Magnesium Alloy

J.D. Bernard[1], J.B. Jordon[2], M.F. Horstemeyer[1,3]
[1]Center for Advanced Vehicular Systems (CAVS), Mississippi State University, Mississippi State, MS 39762
[3]Department of Mechanical Engineering, The University of Alabama, Tuscaloosa, AL 35487
[2]Department of Mechanical Engineering, Mississippi State University, Mississippi State, MS 39762

Keywords: fatigue, replica, AZ61 magnesium alloy, fatigue modeling

Abstract

The purpose of this paper is to quantify the microstructurally small/physically small crack growth behavior in an extruded AZ61 magnesium alloy. Fully-reversed, interrupted load control tests were conducted on notched specimens that were taken from a magnesium alloy extrusion. In order to measure crack growth, replicas of the notch surface were made using a two-part silicon-rubber compound at periodic cyclic intervals. Scanning electron microscopy analysis of the replica surfaces revealed multi site crack initiation and subsequent crack coalescence. The crack growth behavior of the small fatigue cracks was shown to have a strong dependence on the material microstructure as the crack was submitted to a tortuous growth path along grain boundaries and crystallographic slip planes. A microstructurally dependent crack growth model that was previously developed for FCC metals was further extended here to HCP metals.

Introduction

Magnesium alloys are currently being targeted as a potential lightweight metal for widespread use in automotive structural components for the purpose of reducing vehicle weight while maintaining equivalent performance. Although the majority of magnesium alloys that have been researched for use within the automotive industry are cast, extruded magnesium alloys have been shown to exhibit better properties with regards to strength [1]. This is largely because cast products contain microstructural defects like gas pores, pore shrinkage clusters, and oxide films. As such, these microstructural defects can serve as fatigue crack initiation sites and thus reduce the overall fatigue resistance of that alloy. Due to the processing nature, wrought materials lack these defects [2], but they can exhibit anisotropic characteristics and behavior based on loading orientation relative to the process direction (i.e. rolling direction, extrusion, etc) [3]. Since magnesium alloys are naturally anisotropic due to their hexagonal close-packed (HCP) systems which limit the number of potential slip systems that are readily activated [4], extruded magnesium alloys typically have a strong dependence upon loading orientation with respect to the extrusion direction. With regards to characterizing the fatigue behavior of the AZ61 magnesium alloy, previous research has been fairly limited to studying the effects on fatigue by the manganese content, texture, and environmental aspects [5-7]. Furthermore, to the authors' knowledge, studies on the small fatigue crack characteristics on the AZ61 alloy does not exist. Suresh [8] acknowledged the importance of studying small fatigue cracks because a microstructurally small fatigue crack does not necessarily adhere to the more classical approaches of fatigue that are based upon continuum mechanics and linear elastic fracture mechanics [8]. Regarding past studies on other magnesium alloys, Gall *et al.* [9-11] conducted in-situ fatigue tests on cast AM60 magnesium specimens in order to quantify small crack growth behavior. These tests revealed that the material microstructure had a large impact on fatigue crack growth, including that of the small crack nature. They found that fatigue cracks initiated from inclusions, grain boundaries, and persistent slip bands. In the AM60 alloy, the fatigue cracks grew along grain boundaries that contributed to the tortuous crack path. The grain boundaries, in affect, contributed to a varying driving force that resulted in accelerated and retarded crack growth rates.

Initially developed for cast aluminum alloys [12,13], the MultiStage Fatigue (MSF) model was further expanded by Xue *et al.* [14-16] to capture the fatigue characteristics and behavior of LENS shaped steels, wrought aluminum alloys, as well as cast magnesium alloys. However, the small crack formulation of the MSF model has not been verified for wrought magnesium alloys. Thus, the purpose of this paper is quantify the small fatigue crack growth, through the use of the replica method and correlate it to the small crack stage in the MSF model.

Materials and Experimental Methods

The material used in the study is an extruded AZ61 magnesium alloy. The as-received air-quenched extruded alloy is in the form of an automotive crash rail with the cross-section shown in Figure 1a and the specimen layout in Figure 1b. The crash rail was extruded at an average temperature of 500 °C and an extrusion exit speed of 1.2 m/min. The weight percent composition of the AZ61 magnesium alloy is given in Table 1. The as-received material was examined with an optical microscope to quantify the initial microstructure in both a transverse material orientation (Figure 2a) and an extrusion or longitudinal orientation (Figure 2b). X-ray diffraction (XRD) was also performed to quantify texture of the as-received material and the results are shown in Figure 3.

Table 1. AZ61 Chemical Composition by Weight Percent

Al	Zn	Fe	Ni	Cu	Si	Mn
5.85	0.83	0.023	0.0019	0.0057	0.027	0.326

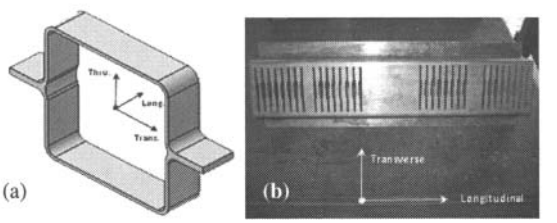

Figure 1. (a) Geometry of the as-received, extruded AZ61 magnesium alloy crash rail and (b) specimen layout rail.

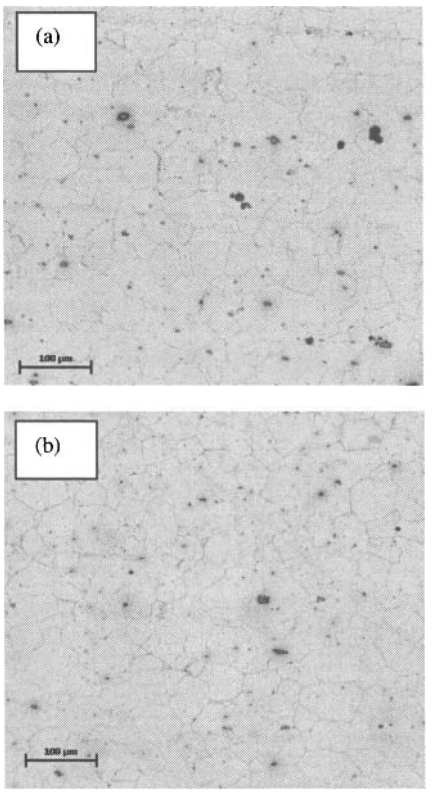

Figure 2. Optical micrographs of the as-received extruded AZ61 magnesium alloy polished and etched: (a) longitudinal orientation (b) transverse orientation.

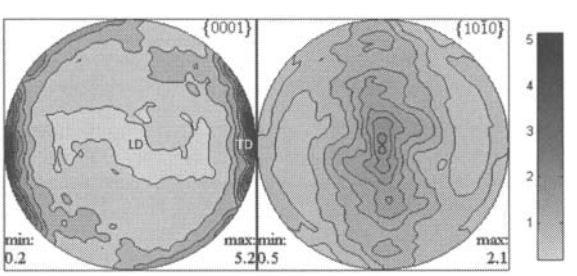

Figure 3. Pole figures of the longitudinal orientation calculated from X-ray diffraction for an AZ61 magnesium alloy.

As previously stated, rectangular cross-sectional fatigue specimens were machined from the crash rail in the transverse orientation as shown in Figure 1b. The specimen design and dimensions are shown in Figure 4. In order to make small fatigue crack growth measurements, a location favorable for crack initiation was required; therefore, a 35mm radius was machined to a depth of 300μm onto the specimen surface according to similar methods found in literature [17]. The shoulder, gage, and notch surfaces of each specimen were hand ground using 800grit sandpaper parallel to the loading direction. In addition to sanding with 800grit sandpaper, several specimens were also polished with a series of 1200grit, 9μm, 6μm, 1μm, and 0.25μm diamond pastes and then polished with OPS, a silicon dioxide (SiO_2) suspension that also mildly etched the specimen surfaces similar to [9-11]. All specimens were then degreased using ethanol. Fully-reversed, load control tests were then conducted to failure on these notched specimens. In addition, several specimens that were ground were fatigue tested but were interrupted at set intervals in order to take replicas of the notch bore. The replicas were made by using a dual-part silicone based compound, called Repliset®. The Repliset® compound has a resolution 0.1μm, but must be sputter coated with gold palladium for optimal SEM image observation. All replicas were sputter coated for a period of 30 seconds. Upon failure, the fracture surfaces were cut off from the specimen and mounted for SEM examination for further fractography analysis.

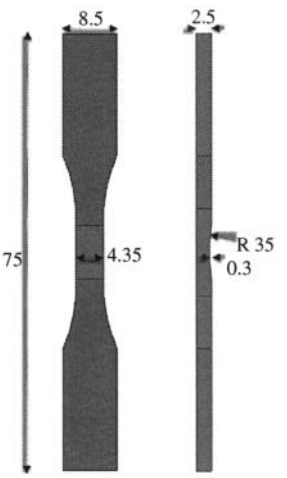

Figure 4. Fatigue specimen geometry, all dimensions are in mm.

Fatigue Life Results of Notched Specimens

The stress-life values were plotted for the failed specimens in order to determine what significance the surface preparation and replication had upon the overall fatigue life. The results are shown in Figure 5.

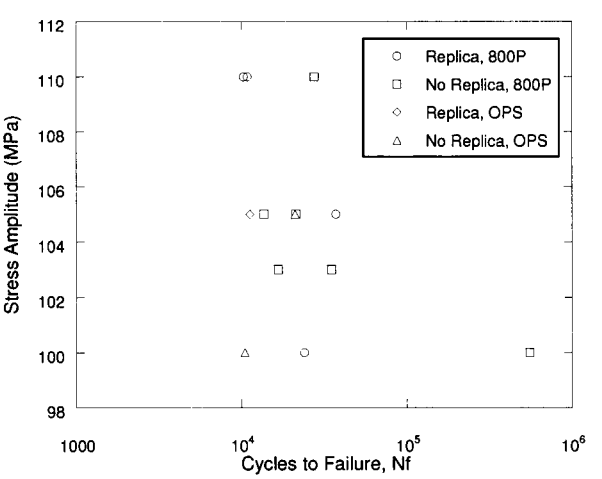

Figure 5. Stress amplitude versus cycles to failure for the specimens tested.

Note that in Figure 5, the circles indicate specimens prepared by sanding with 800grit sandpaper and had replicas taken of the notch. The boxes indicate specimens that were sanded with 800grit, but with no replicas taken. The diamonds indicates OPS specimens with no replicas. Although there is some scatter in the above plot, neither replicating the surface of the specimen nor preparing them with OPS had a profound or consistent impact upon the fatigue life of the specimens.

Small Fatigue Crack Behavior

Using SEM imaging of the replicas, the fatigue crack initiation and growth on the notch surface were experimentally observed. Each replica was observed in the SEM starting with the last replica prior to failure. Once the dominate fatigue crack was located and measured, each preceding replica was examined and the length of the dominate crack was measured until the crack was no longer visible. Figure 6 presents the crack length versus number of cycles. For this particular specimen, the load amplitude was 105MPa (R=-1) and replicas were taken at intervals of 1,000 cycles. Also indicated in Figures 6, 7, and 8 are the points A, B, and C which correspond to cycles 13,000, 19,000, and 24,000, respectively.

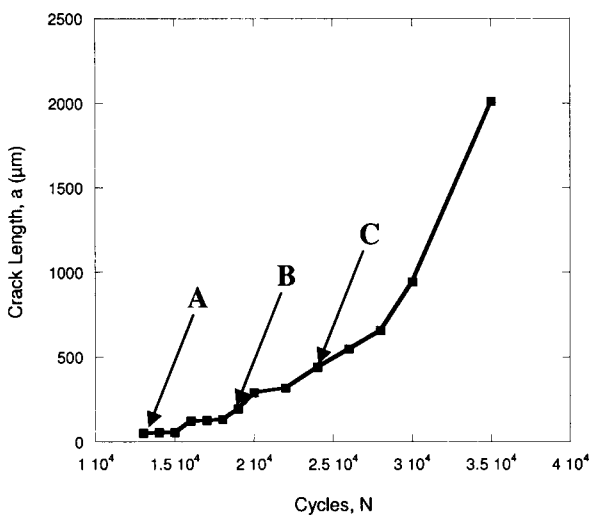

Figure 6. Crack length versus cycles for a stress amplitude of 105MPa

Upon plotting the crack growth rate versus crack length, shown in Figure 7, there is a marked acceleration/deceleration between points A and B which results in the corresponding crack growth from 13,000 cycles to 19,000 cycles. This is likely due to grain boundary blocking where the crack, outlined in Figure 8, grew through and around grain boundaries. Note that this specimen surface was prepared with 800 grit sandpaper and the roughness shown in Figure 8 is from the grinding process. Between points B and C, however, driving force increased such that the growth rate become more constant. This is likely because as the crack grew in length, the driving force increased such that the crack path became less dependent on the crystallographic orientation, and thus rendered it less sensitive to the material microstructure.

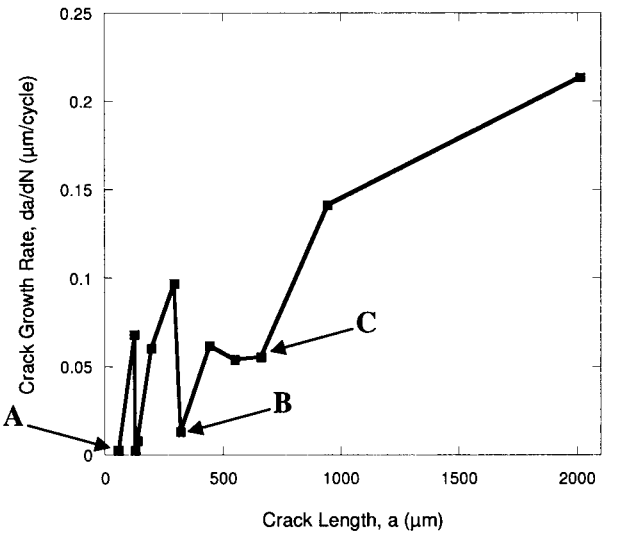

Figure 7. Crack growth rate versus crack length for a stress amplitude of 105MPa.

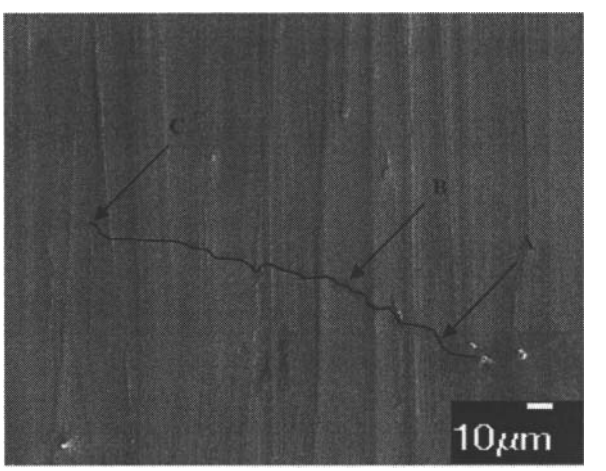

Figure 8. Replica image illustrating the path of the crack shown in Figures 6 and 7, along with the locations of the indicated points.

Previous research conducted by Gall *et al.* [9-11] on cast magnesium showed that the microstructurally small cracks had a strong dependence on the material microstructure. Features such as dendrites and particle laden interdendritic regions demonstrated a significant impact on the small crack growth rate. Although the extruded magnesium alloy examined in this paper had a different microstructure than the cast AM60B previously researched, parallels between the two studies can still be drawn. Small fatigue cracks were shown to preferentially propagate through favorably oriented dendrites in cast magnesium and grains in the extruded AZ61 magnesium alloy. In addition, the smaller fatigue cracks displayed a stronger dependence upon the material microstructure than longer fatigue cracks in both the cast and extruded magnesium materials.

Finite Element Analysis of Notched Specimen

In order to correlate the small fatigue crack stage of the MSF model to crack growth data, the local stress state was needed. Since the notched specimen creates a slightly non-uniaxial stress state, finite element analysis (FEA) of the specimen was conducted to determine the stress state of the notch under cyclic loading. As such, a non-linear finite element material model was employed. The material model used in the FEA is the plasticity-damage internal state variable (ISV) model first developed by Bammann *et al.* [18-20] and later modified by Horstemeyer *et al.* [21,22]. For a complete description of the ISV model, see [18-22]. The material model constants were determined based on monotonic tensile and compression tests. Three-dimensional finite element simulations of the entire notched specimen were performed using the aforementioned constitutive model. The boundary conditions employed in this study were identical to the ones employed in the experiment. In order to satisfy continuum mechanics conditions, the 8-node brick element used in the notch bore region was less than ten times the size of the average grain size of the magnesium AZ61 alloy.

A relationship between equivalent stress at the notch root and remote loading were determined from the FEA, as shown in Figure 9. The relationship between local equivalent stress became non-linear due to local plastic deformation in the notch.

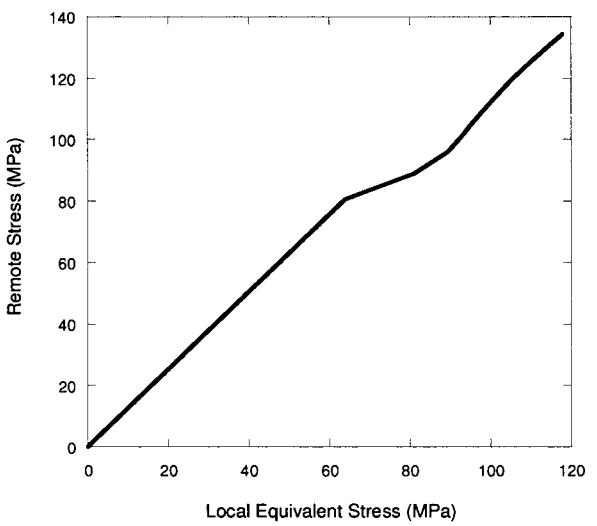

Figure 9. Local equivalent stress as a function of the remote stress for the notched specimens.

Small Fatigue Crack Model

To provide context for the small crack fatigue stage of the model, an overview of the MSF model is presented. The MSF model [12] divides the total fatigue life into three distinct regions: incubation, microstructurally small/physically small crack growth, and long crack growth, as shown in Eq. 1.

$$N_{\text{Total}} = N_{\text{Inc}} + N_{\text{MSC/PSC}} + N_{\text{LC}} \tag{1}$$

where N_{Total} is the total fatigue life. N_{Inc} is the number of cycles required to incubate a crack from an inclusion. In the case of the magnesium alloy, the inclusion is an intermetallic particle. The incubated crack then expands from the inclusion into the matrix. $N_{\text{MSC/PSC}}$ is the number of cycles required to propagate a crack through the microstructurally small/physically small crack regime. Finally, N_{LC} is number of cycles of long crack (LC) propagation to final failure, which depends on the amplitude of loading and the corresponding extent of plasticity ahead of the crack tip.

The MSC/PSC model is a function of the crack tip displacement (Eq. 2) and portrays the small crack growth regime, where ΔCTD is the crack tip displacement range, χ is a material constant, and ΔCTD_{th} is the range of the threshold for crack tip displacement. χ is 0.32 for aluminum alloys and has been taken as this value for the given material.

$$\left(\frac{da}{dN}\right)_{msc} = \chi\left(\Delta CTD - \Delta CTD_{th}\right) \tag{2}$$

The range of the crack tip displacement, shown in Eq. (3), is a function of remote loading where C_I, C_{II}, ξ, ξ', ω, ω', and ζ are constants based on small crack growth experiments.

$$\Delta CTD = C_{II}\left(\frac{GS}{GS_0}\right)^{\varpi}\left(\frac{GO}{GO_0}\right)^{\xi}\left[\frac{U\Delta\hat{\sigma}}{S_{ut}}\right]^{\zeta} a + C_I\left(\frac{GS}{GS_0}\right)^{\varpi'}\left(\frac{GO}{GO_0}\right)^{\xi'}\left[\frac{\Delta\gamma^p_{\max}}{2}\Big|_{macro}\right]^2 \tag{3}$$

The ratio of grain size to the reference grain size of the material, shown as $\left(\frac{GS}{GS_0}\right)$, represents the effect of grain size distribution upon the small crack growth. The ratio of the Taylor factor for the orientation of the grain at the crack tip with the Taylor factor of the typical rolling texture, $\left(\frac{GO}{GO_0}\right)$, encompasses the effect of texture upon the MSC growth regime. The nonlocal maximum plastic shear strain amplitude term, represented by $\left(\frac{\Delta\gamma^P max}{2}\right)$ in Equation 3, can be found by Equation 4,

$$C_{inc}N_{inc}^{\alpha} = \beta = \frac{\Delta\gamma^P_{\max}}{2} \tag{4}$$

where N_{inc} is the number of cycles required to incubate a crack, α is a material constant that is based on the macroscopic Coffin-Manson law, and C_{inc} can be solved by using the following equation. The constants related to the Coffin-Manson law were based on strain-life experiments of magnesium AZ61 alloy of Gibson *et al.* [23].

Small Fatigue Crack Model Correlation

The small crack equations presented here were used to make correlations to the crack growth rate measured in the interrupted tests. The small crack model was plotted as a function of crack length and subsequently compared to the crack growth data, shown in Figure 10. It is important to note that the small crack model (Equation 2) is intended to model crack growth for a through crack of crack length, a. In this study, the experimental

small crack measurements were taken from surface crack growth. For the correlation process, we assume that the crack grew in a symmetric semi-circular shape and the surface crack length (c) is equal to twice the depth of the crack length (2a). Thus, we correlated the small crack model to ½ of the surface crack length, c, in which we measured the crack growth rate to the left of the initiation site as shown in Figure 7. Although the model captured the mean trend of the crack growth rate, the scatter in the data is quite significant when the crack is less than 500 μm in length. While not shown here, the small crack model can be used to predict the upper and lower bounds of the crack growth rate data.

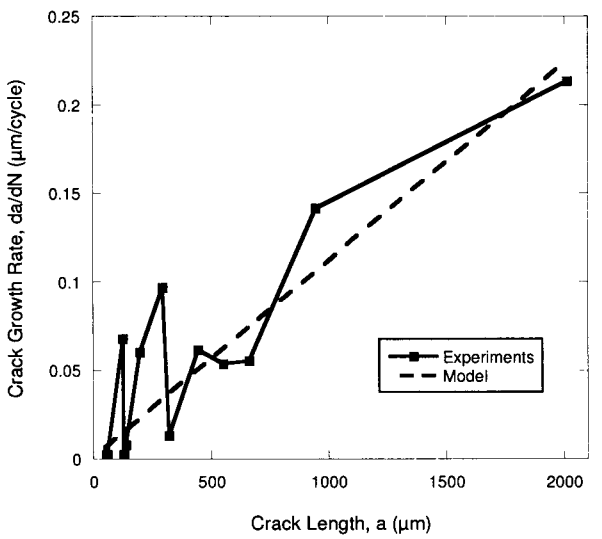

Figure 10. Crack growth rate versus crack length for a stress amplitude of 105MPa with the model approximations also shown.

Summary

Based on the small fatigue crack experiments and modeling presented here, we present the following summary:

1. Surface preparation and replicas taken of the notch surface had no notable impact upon the fatigue life of the material.

2. The replica method was able to capture the mean crack growth of the AZ61 material, particularly within the microstructurally small/physically small crack regime.

3. The small crack equations of the multistage fatigue model were correlated to the small crack growth behavior of the AZ61 alloy.

4. Small fatigue cracks were shown to preferentially propagate through favorably oriented grains in the extruded AZ61 magnesium alloy.

5. When the crack was small, (less than 500μm), the fatigue crack displayed a stronger dependence upon the material microstructure compared to when it was longer in length.

Acknowledgments

The authors would like to recognize Richard Osborne, James Quinn, Xuming Su, John Allison, Robert McCune, Don Penrod, and Matthew Castanier for their encouragement of this study. This material is based upon work supported by the Department of Energy and the National Energy Technology Laboratory through a subcontract with Mississippi State University, and was performed for the Simulation Based Reliability and Safety (SimBRS) research program. This report was prepared as an account of work sponsored by an agency of the United States Government. Neither the United States Government nor any agency thereof, nor any of their employees, makes any warranty, express or implied, or assumes any legal liability or responsibility for the accuracy, completeness, or usefulness of any information, apparatus, product, or process disclosed, or represents that its use would not infringe privately owned rights. Reference herein to any specific commercial product, process, or service by trade name, trademark, manufacturer, or otherwise does not necessarily constitute or imply its endorsement, recommendation, or favoring by the United States Government or any agency thereof. The views and opinions of authors expressed herein do not necessarily state or reflect those of the United States Government or any agency thereof. Such support does not constitute an endorsement by the Department of Energy of the work or the views expressed herein. UNCLASSIFIED: Dist A. Approved for public release.

References

1. S. Begum, D.L. Chen, S. Xu, and Alan A. Luo, "Strain-Controlled Low-Cycle Fatigue Properties of a Newly Developed Extruded Magnesium Alloy," *Metallurgical and Materials Transactions A*, 39A (2008), 3014-3026.

2. F. Yang, S.M. Yin, S.X. Li, and Z.F. Zhang, "Crack initiation mechanism of extruded AZ31 magnesium alloy in the very high cycle fatigue regime," *Materials Science and Engineering A*, 491 (2008), 131-136.

3. J.B. Jordon, M.F. Horstemeyer, K. Solanki, J.D. Bernard, J.T. Berry, T.N. Williams, "Damage characterization and modeling of a 7075-T651 aluminum plate," *Materials Science and Engineering A*, 527 (2009), 169-178.

4. S. Begum, D.L. Chen, S. Xu, Alan A. Luo, "Effect of strain ratio and strain rate on low cycle fatigue behavior of AZ31 wrought magnesium alloy," *Materials Science and Engineering A*, 517 (2009) 334-343.

5. Z.B. Sajuri, Y. Miyashita, Y. Hosokai, Y. Mutoh, "Effects of Mn content and texture on fatigue properties of as-cast and extruded AZ61 magnesium alloys," *International Journal of Mechanical Sciences*, 48 (2) (2006) 198-209.

6. K. Tokaji, M. Nakajima, Y. Uematsu, "Fatigue crack propagation and fracture mechanisms of wrought magnesium alloys in different environments," *International Journal of Fatigue*, 31 (7) (2009) 1137-1143.

7. Z.B. Sajuri, Y. Miyashita, Y. Mutoh, "Effects of humidity and temperature on the fatigue behaviour of an

extruded AZ61 magnesium alloy," *Fatigue and Fracture of Engineering Materials and Structures*, 28, 4 (2005) 373-379.

8. S. Suresh, "Fatigue of Metals," Cambridge University Press, Cambridge, 1998.
9. K. Gall, G. Biallas, Hans J. Maier, P. Gullett, M. F. Horstemeyer, D. L. McDowell, and J. Fan, "In-situ observations of high cycle fatigue mechanisms in cast AM60B magnesium in vacuum and water vapor environments," *International Journal of Fatigue*, 26 (2004) 59-70.
10. K. Gall, G. Biallas, H. J. Maier, M. F. Horstemeyer, and D. L. McDowell, "Environmentally influenced microstructurally small fatigue crack growth in cast magnesium," *Materials Science and Engineering A*, 396 (2004) 143-154.
11. K. Gall, G. Biallas, H. J. Maier, P. Gullett, M. F. Horstemeyer, and D. L. McDowell, "In-Situ Observations of Low-Cycle Fatigue Damage in Cast AM60B Magnesium in an Environmental Scanning Electron Microscope," *Metallurgical and Materials Transactions* A, 35 (2004) 321-331.
12. D.L. McDowell, K. Gall, M.F. Horstemeyer, and J. Fan, "Microstructure-based fatigue modeling of cast A356-T6 alloy," *Engineering Fracture Mechanics,* 70 (1) (2003), 49-80.
13. J.B. Jordon, M.F. Horstemeyer, N. Yang, J.F. Major, K.A. Gall, J. Fan, D.L. McDowell, "Microstructural inclusion influence on fatigue of a cast A356 aluminum alloy," *Metallurgical and Materials Transactions* A, 41A (2) (2010), 356-363.
14. Y. Xue, A. Pascu, M.F. Horstemeyer, L. Wang, P.T. Wang, "Microporosity effects on cyclic plasticity and fatigue of LENS™-processed steel," Acta Materialia 58 (11) (2010), 4029-4038.
15. Y. Xue, D.L. McDowell, M.F. Horstemeyer, M.H. Dale, J.B. Jordon, "Microstructure-based multistage fatigue modeling of aluminum alloy 7075-T651," *Engineering Fracture* Mechanics, 74 (17) (2007), 2810-2823.
16. Y. Xue, M.F. Horstemeyer, D.L. McDowell, H. El Kadiri, J. Fan, "Microstructure-based multistage fatigue modeling of a cast AE44 magnesium alloy," *International Journal of Fatigue*, 29 (4) (2007), 666-676.
17. K. Tokaji, M. Kamakura, Y. Ishiizumi, N. Hasegawa, "Fatigue behaviour and fracture mechanism of a rolled AZ31 magnesium alloy," *International Journal of* Fatigue, 26 (11) (2004), 1217-1224.
18. D.J. Bammann, "Internal variable model of viscoplasticity," *International Journal of Engineering Science*, 22 (8-10) (1983), 1041-1053.
19. D.J. Bammann, E.C. Aifantis, "Model for finite-deformation plasticity," Acta *Mechanica*, 69 (1-4) (1987), 97-117.
20. D.J. Bammann, E.C. Aifantis, "A damage model for ductile metals," *Nuclear Engineering and Design*, 116 (3) (1989), 355-362.
21. M.F. Horstemeyer, A.M. Gokhale, "Void-crack nucleation model for ductile metals," *International Journal of Solids and Structures*, 36 (33) (1999), 5029-5055.
22. M.F. Horstemeyer, J. Lathrop, A.M. Gokhale, M. Dighe, "Modeling stress state dependent damage evolution in a cast Al-Si-Mg aluminum alloy," *Theoretical and Applied Fracture Mechanics*, 33 (1) (2000), 31-47.
23. J.B. Jordon, J.B. Gibson, M.F. Horstemeyer, "Experiments and Modeling of Fatigue Damage in Extruded Mg AZ61 Alloy," *TMS Annual Meeting and 2011*, Submitted.